

## Self-Assembly of Nonionic Surfactants into Lyotropic Liquid Crystals in Ethylammonium Nitrate, a Room-Temperature Ionic Liquid

Miguel U. Araos and Gregory G. Warr\*

*School of Chemistry, University of Sydney, Sydney, NSW, 2006, Australia*

*Received: May 30, 2005*

The stability of a variety of lyotropic liquid crystals formed by a number of polyoxyethylene nonionic surfactants in the room-temperature ionic liquid ethylammonium nitrate (EAN) is surveyed and reported. The pattern of self-assembly behaviour and mesophase formation is strikingly similar to that observed in water, even including the existence of a lower consolute boundary or cloud point. The only quantitative difference from water is that longer alkyl chains are necessary to drive the formation of liquid crystalline mesophases in EAN, suggesting that a rich pattern of “solvophobic” self-assembly should exist in this solvent.

### Introduction

Over the past several years, there has been an upsurge in interest in room-temperature ionic liquids, or molten salts, as solvents for organic and inorganic synthesis, largely focused on imidazolium derivatives. This has mainly been based around their “green” pedigree, due to their negligible vapor pressure, and to their tunability as solvents by ready incorporation of one or more functional groups.<sup>1–3</sup> There are a few recent studies of surfactant behavior in such ionic liquids, but the amount of attention paid to this is miniscule compared with the burgeoning literature on synthesis.

Up to the present, the evidence in favor of surfactant self-assembly in imidazolium ionic liquids is ambiguous at best.<sup>4,5</sup> Micelles have not been definitively shown to exist in such ionic liquids, although one recent report shows the first strong evidence for vesicle formation in an ether-containing ionic liquid, making a strong case for purely “ionophobic” surfactant self-assembly.<sup>6</sup>

Ethylammonium nitrate (EAN) is a room-temperature ionic liquid whose behavior is in striking contrast to more widely studied ionic liquids. Self-assembly of surfactants into micelles<sup>7,8</sup> and of lipids into lamellar liquid-crystal phases<sup>9–11</sup> in EAN was clearly demonstrated to occur over twenty years ago. Unlike most ionic liquids of current interest, EAN has the potential to form a three-dimensional hydrogen-bond network, and this was postulated to be an essential feature in supporting self-assembly.<sup>12</sup>

In this paper, we explore more fully solvophobic self-assembly by nonionic surfactants in EAN. Using polyoxyethylene surfactants,  $C_nE_m$ , with a range of alkyl and ethoxy chain lengths so that molecular structure is systematically varied, we map out the kinds of lyotropic phases formed and relate this to their well-known behavior in aqueous systems. We have also chosen these nonionic surfactants particularly as they address this central issue of the role of H-bonding in solvophobic self-assembly. Their polyether hydrophilic moiety has at least

the potential to be solvated by the H-bonding to the ethylammonium cation, giving them a stronger amphiphilic character in EAN than in non-hydrogen-bonding ionic liquids. Nonionic surfactants are also chosen because they are free of counterion effects, which can have a strong influence on self-assembly in water and nonaqueous solvents. For example, in a study of the phase behavior of cationic alkylpyridinium surfactants in a variety of nonaqueous solvents, cubic phases were not found to form in EAN, and this was attributed to specific ion effects.<sup>13</sup>

### Experimental Section

Polyoxyethylene alkyl ether nonionic surfactants,  $C_nE_m$ , of various alkyl chain lengths,  $n$ , and degrees of ethoxylation,  $m$ , were purchased from Nikkol or Fluka and were used as received. Purity was verified by reverse-phase high-purity liquid chromatography (HPLC).

Ethylammonium nitrate (EAN) was prepared as described previously,<sup>7</sup> by slow addition of concentrated nitric acid to ethylamine solution chilled in ice. The product was rotary-evaporated and then freeze-dried to remove water, and then stored under nitrogen. Its melting point was determined to be 14 °C, in good agreement with previous reports.<sup>7</sup> The water content, determined by Karl Fischer titration, was around 0.7% v/v.

Lyotropic phase formation was first identified by diffusive interfacial transport, or “flooding” experiments, in which a concentration gradient is established by contacting surfactant and EAN under a polarizing optical microscope.<sup>14</sup> Nematic, hexagonal, and lamellar phases were identified by their optical textures, following well-established practice.<sup>15</sup> Cubic phases were identified in flooding experiments by the presence of faceted or highly distorted bubbles in an optically isotropic continuum. Using a heating stage operating up to 62.5 °C, we identified the maximum temperatures at which each phase was stable in these gradient samples.

Two samples with particularly rich phase behavior were further investigated using the sequential dilution technique of Laughlin,<sup>16</sup> in which a binary mixture is temperature-cycled and

\* Author for correspondence: g.warr@chem.usyd.edu.au.

**TABLE 1: Summary of Lyotropic Phases Observed in  $C_nE_m$ -EAN Binary Mixtures, Including the Melting Temperature of the Phase Or, in the Case of the  $L_1$  Phase, the Cloud Point (lower consolute temperature) of a 5 wt % Solution**

|             | $L_1$          | $I_1$        | $H_1$        | $V_1$    | $L_\alpha$   | solid |
|-------------|----------------|--------------|--------------|----------|--------------|-------|
| $C_{12}E_5$ | <i>a</i>       | <i>b</i>     | <i>b</i>     | <i>b</i> | <i>b</i>     | 24 °C |
| $C_{12}E_6$ | <i>a</i>       | <i>b</i>     | <i>b</i>     | <i>b</i> | <i>b</i>     | 25 °C |
| $C_{12}E_8$ | <i>a</i>       | <i>b</i>     | <i>b</i>     | <i>b</i> | <i>b</i>     | 31 °C |
| $C_{14}E_4$ | $T_c = 49$ °C  | <i>b</i>     | <i>b</i>     | <i>b</i> | $\sim 50$ °C | 29 °C |
| $C_{14}E_6$ | <i>a</i>       | <i>b</i>     | <i>b</i>     | <i>b</i> | <i>b</i>     | 35 °C |
| $C_{14}E_8$ | <i>a</i>       | <i>b</i>     | $\sim 30$ °C | <i>b</i> | <i>b</i>     | 38 °C |
| $C_{16}E_4$ | $T_c = 88$ °C  | <i>b</i>     | <i>b</i>     | <i>b</i> | $> 60$ °C    | 35 °C |
| $C_{16}E_6$ | $T_c = 130$ °C | 40 °C        | 67 °C        | 48 °C    | <i>b</i>     | 37 °C |
| $C_{16}E_8$ | <i>a</i>       | <i>b</i>     | $> 60$ °C    | <i>b</i> | <i>b</i>     | 42 °C |
| $C_{18}E_2$ | $T_c = 74$ °C  | <i>b</i>     | <i>b</i>     | <i>b</i> | $> 50$ °C    | 45 °C |
| $C_{18}E_4$ | $T_c = 105$ °C | <i>b</i>     | <i>b</i>     | <i>b</i> | $> 50$ °C    | 41 °C |
| $C_{18}E_6$ | $T_c = 123$ °C | $\sim 35$ °C | 60 °C        | 56 °C    | 96 °C        | 48 °C |
| $C_{18}E_8$ | <i>a</i>       | $\sim 40$ °C | $> 60$ °C    | 45–50 °C | 55–60 °C     |       |

<sup>a</sup> A 5 wt % solution of the surfactant did not demix up to 130 °C.

<sup>b</sup> A particular phase was not observed in the temperature range investigated.

observed under crossed polarizers to determine the phases formed. The sample is then diluted repeatedly with solvent and cycled at each composition until a new set of equilibrium phases and transition temperatures is identified. To reduce errors from serial dilutions, the phase diagrams shown include dilution data from a series of overlapping starting compositions. Individual samples were also prepared, especially to check for mesophases that are stable over only a narrow composition range. A broader temperature range was examined in these samples than was possible on our heating stage. Cloud points were determined by observing 1% and 5% solutions in EAN as they were cycled between room temperature and 130 °C.

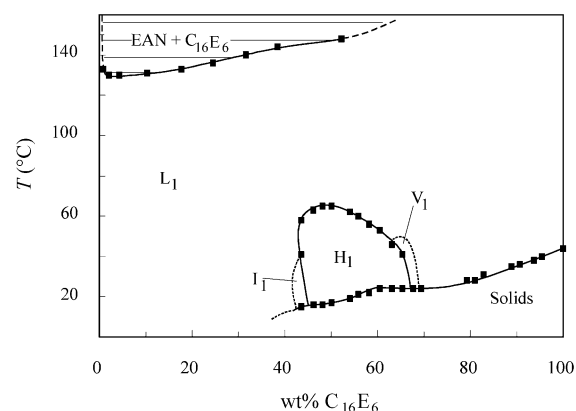
## Results and Discussion

Table 1 summarizes our observations of the binary phase equilibria for nonionic surfactants  $C_nE_m$ -EAN mixtures. Typical surfactants for aqueous applications with dodecyl chains are completely miscible with EAN, and those examined formed no lyotropic phases at any compositions. In the flooding experiments, the solids dissolved into an isotropic liquid, or in the case of  $C_{12}E_5$ , the liquid surfactant and EAN simply mixed. Of course, this does not rule out the formation of micelles in the dodecyl-chained surfactants.

Tetradecyl surfactants showed some evidence of lyotropic phase formation. A lamellar phase is observed for  $C_{14}E_4$  and a poorly defined hexagonal (or possibly nematic) texture for  $C_{14}E_8$ . Both are stable only at quite low temperatures.

The formation of a range of lyotropic phases familiar from aqueous surfactant chemistry begins to occur with hexadecyl-chained surfactants. Polyoxyethylene hexadecyl- and octadecyl-ethers both exhibit the full range of common lyotropic mesophases including  $L_1$  liquid isotropic, presumed to be micellar,  $I_1$  discrete cubic,  $H_1$  direct hexagonal,  $V_1$  bicontinuous cubic, and  $L_\alpha$  lamellar phases. We have not identified the formation of other liquid isotropic phases ( $L_2$ , etc.) in Table 1, but see below. The melting point, or maximum temperature where the phase is found to be stable, is listed in Table 1. Where temperature ranges are given, these indicate the temperature interval between isothermal flooding experiments.

Hexadecyl and octadecyl surfactants also exhibit behavior typical of a Krafft boundary.<sup>17</sup> Below a certain temperature, well below the surfactant's melting point, solvated surfactant crystals coexist with a dilute EAN solution. Liquid crystalline phases are only observed above this boundary.



**Figure 1.** Phase diagram of the binary  $C_{16}E_6$ -EAN system, showing a large single-phase isotropic ( $L_1$ ) region, together with discrete cubic, hexagonal, bicontinuous cubic, and lamellar phases. Dashed lines indicate approximate phase boundaries determined for the smaller lyotropic phases, and horizontal hatching denotes tie lines for two-phase coexistence.

Figure 1 shows the phase diagram of the binary  $C_{16}E_6$ -EAN system determined using the serial dilution technique of Laughlin.<sup>16</sup> There is a broad range of complete miscibility of molten  $C_{16}E_6$  and EAN between 67 and 130 °C. Between 16 and 67 °C, a large hexagonal ( $H_1$ ) phase is evident in the middle of the composition range, and at higher surfactant concentrations, a bicontinuous cubic ( $V_1$ ) phase forms over a narrow composition range. The  $V_1$  phase is clearly evident in surfactant flooding experiments, but the compositions of its phase boundaries have so far only been determined approximately. In some flooding experiments, we also detected an optical texture consistent with a lamellar ( $L_\alpha$ ) phase at higher concentration than the  $V_1$ , up to about 40 °C. If present at equilibrium, this phase has only a very small stability region and is omitted from the table and figure until it is verified.

The Krafft boundary, separating solid and liquid or liquid crystalline phases, drops below room temperature for compositions below 40 wt %  $C_{16}E_6$ . Recall that EAN itself melts at 14 °C, so this region and further details such as the location of the eutectic point were not investigated.

At higher temperatures,  $C_{16}E_6$  and EAN demix into surfactant-rich and dilute solutions. This behavior is highly reminiscent of the well-known cloud-point phenomenon in aqueous surfactant and poly(ethylene oxide) solutions, but occurs here at much higher temperature. Like aqueous surfactant solutions, the critical composition is very dilute, indicating the presence of large aggregates.<sup>18</sup>

Figure 2 shows the phase diagram of the binary  $C_{18}E_6$ -EAN system. Like the  $C_{16}E_6$ -EAN system, a rich sequence of lyotropic mesophases occurs, including hexagonal, bicontinuous cubic, and lamellar phases. There is some indication of a small  $I_1$  discrete cubic phase from the shape of the  $H_1$ - $L_1$  phase boundary near the Krafft boundary and from flooding experiments, but we have not yet isolated this phase. Again, a liquid-liquid miscibility gap with a cloud point is observed in this system. The Krafft boundary for this surfactant is higher, and the  $L_1$  phase only forms above about 37 °C at high concentrations.

The pattern of phase behaviour of polyoxyethylene nonionic surfactants in EAN is remarkably similar to that elucidated by Mitchell et al. for this class of nonionic surfactants in water over twenty years ago.<sup>19</sup> The phase diagrams of  $C_{16}E_6$ -EAN and  $C_{18}E_6$ -EAN, for example, closely resemble those of  $C_{12}E_8$ -H<sub>2</sub>O and  $C_{12}E_6$ -H<sub>2</sub>O, respectively.

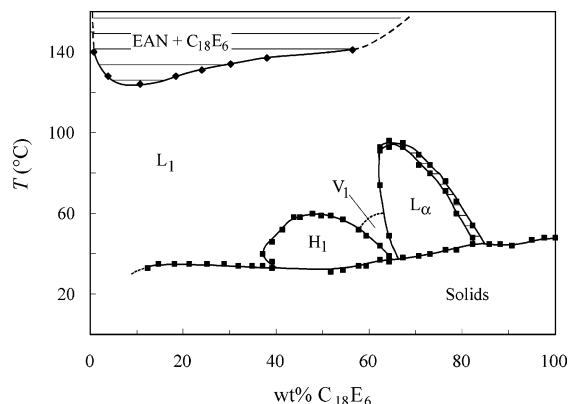


**Figure 2.** Phase diagram of the binary  $C_{18}E_6$ -EAN system, showing a large single-phase isotropic ( $L_1$ ) region, together with hexagonal, bicontinuous cubic, and lamellar phases. Dashed lines indicate approximate phase boundaries determined for the smaller lyotropic phases, and horizontal hatching denotes tie lines for two-phase coexistence.

Not only do the sequence of phases formed in each binary mixture follow expectations for aqueous systems, but so do the trends with changing alkyl and ethoxy chain lengths. For the octadecyl chains, we observe only lamellar phases for the surfactants with the smallest solvophilic ethoxy chains and hence the lowest spontaneous curvature (highest surfactant-packing parameter<sup>20</sup>)  $C_{18}E_2$  and  $C_{18}E_4$ . Increasing ethoxy chain length to  $C_{18}E_6$  produces  $H_1$  and  $V_1$  phases, but these all melt at lower temperatures than  $L_\alpha$ , suggesting that low curvature is still preferred. However, upon increasing ethoxy chain length to  $C_{18}E_8$ , the lamellar phase melts at lower temperature than the hexagonal phase.

The same pattern is repeated in the hexadecyl systems.  $C_{16}E_4$  forms only a lamellar phase;  $C_{16}E_6$  forms a highly stable hexagonal phase flanked at lower and higher concentrations by cubic phases with higher and lower curvature structures;  $C_{16}E_8$  forms only a hexagonal phase (within experimental resolution). Like aqueous systems, for the same ethoxy chain length, shortening the alkyl chain favors higher curvature structures.

Like polyoxyethylene octyl ethers in water,<sup>21</sup> dodecyl non-ionic surfactants in EAN yield no lyotropic phases. Surfactants with tetradecyl chains are intermediate in behavior, forming lyotropic phases that have only narrow temperature stability ranges.

Cloud points also follow the trends observed in aqueous systems, increasing with both alkyl and ethoxy chain lengths.<sup>19</sup> Cloud points were determined in 5 wt % EAN solution (Table 1), as the shape of the lower consolute boundary indicates that the critical concentration is higher than in water (see Figures 1 and 2). With the exception of  $C_{16}E_6$ , 1 wt % EAN solutions of all surfactants studied remained clear at temperatures up to 130

°C. It is somewhat surprising that dodecyl surfactants do not show cloud points, but they may do so at higher concentrations if only small micelles are formed.<sup>22,23</sup>

On the basis of these trends, we would anticipate that a wide variety of other self-assembly phases could be produced relatively easily and at predictable compositions in EAN. For example, a sponge phase should form for  $C_{14}E_m$  or  $C_{16}E_m$ , with  $m = 3-5$  at elevated temperatures.<sup>24,25</sup> Likewise, a ternary mixture of  $C_{12}E_m$ , dodecanol, and EAN should yield lamellar and sponge phases,<sup>21</sup> and microemulsions should form in the presence of an EAN-immiscible hydrophobic solvent.

**Acknowledgment.** This work was supported by the Australian Research Council, the University of Sydney Research Grant Scheme, and Dyno Nobel Asia Pacific.

## References and Notes

- (1) Forsyth, S. A.; Pringle, J. M.; MacFarlane, D. R. *Aust. J. Chem.* **2004**, *57*, 113–119.
- (2) Rogers, R. D.; Seddon, K. R. *Science* **2003**, *302*, 792–793.
- (3) Seddon, K. R.; Stark, A.; Torres, M.-J. *Pure Appl. Chem.* **2000**, *72*, 2275–2287.
- (4) Anderson, J. L.; Pino, V.; Hagberg, E. C.; Sheares, V. V.; Armstrong, D. W. *Chem. Commun.* **2003**, 2444–2445.
- (5) Fletcher, K. A.; Pandey, S. *Langmuir* **2004**, *20*, 33–36.
- (6) Nakashima, T.; Kimizuka, N. *Chem. Lett.* **2002**, 1018–1019.
- (7) Evans, D. F.; Yamauchi, A.; Roman, R.; Casassa, E. Z. *J. Colloid Interface Sci.* **1982**, *88*, 89–96.
- (8) Evans, D. F.; Yamauchi, A.; Wei, G. J.; Bloomfield, V. A. *J. Phys. Chem.* **1983**, *87*, 3537–3541.
- (9) Evans, D. F.; Kaler, E. W.; Benton, W. J. *J. Phys. Chem.* **1983**, *87*, 533–535.
- (10) Tamura-Lis, W.; Lis, L. J.; Quinn, P. J. *J. Phys. Chem.* **1987**, *91*, 4625–4627.
- (11) Tamura-Lis, W.; Lis, L. J.; Quinn, P. J. *Biophys. J.* **1988**, *53*, 489–492.
- (12) Evans, D. F.; Chen, S.-H.; Schriver, G. W.; Arnett, E. M. *J. Am. Chem. Soc.* **1981**, *103*, 481–482.
- (13) Bleasdale, T. A.; Tiddy, G. J. T.; Wyn-Jones, E. *J. Phys. Chem.* **1991**, *95*, 5385–5386.
- (14) Laughlin, R. G. *Adv. Colloid Interface Sci.* **1992**, *41*, 57–79.
- (15) Rosevear, F. B. *J. Am. Oil Chem. Soc.* **1954**, *31*, 628–638.
- (16) Laughlin, R. G. *J. Colloid Interface Sci.* **1976**, *55*, 239–241.
- (17) Laughlin, R. G. *The Aqueous Phase Behavior of Surfactants*; Academic Press: London, 1994.
- (18) Kjellander, R. *J. Chem. Soc., Faraday Trans. II* **1982**, *78*, 2025–2042.
- (19) Mitchell, J. D.; Tiddy, G. J. T.; Waring, L.; Bostock, T.; McDonald, M. P. *J. Chem. Soc., Faraday Trans. II* **1983**, *79*, 975–1000.
- (20) Israelachvili, J. N.; Mitchell, J. D.; Ninham, B. W. *J. Chem. Soc., Faraday Trans. II* **1976**, *72*, 1525–1568.
- (21) Penders, M. H. G. M.; Strey, R. *J. Phys. Chem.* **1995**, *99*, 6091–6095.
- (22) Warr, G. G.; Zemb, T. N.; Drifford, M. *J. Phys. Chem.* **1990**, *94*, 3086–3092.
- (23) Buckingham, S. A.; Garvey, C. J.; Warr, G. G. *J. Phys. Chem.* **1993**, *97*, 10236.
- (24) Le, T. D.; Olsson, U.; Mortensen, K.; Zipfel, J.; Richtering, W. *Langmuir* **2001**, *17*, 999–1008.
- (25) Lang, J. C.; Morgan, R. D. *J. Chem. Phys.* **1980**, *73*, 5849–5861.